



## Get Clarity On Generics

Cost-Effective CT & MRI Contrast Agents

 FRESENIUS  
KABI

WATCH VIDEO

# AJNR

This information is current as  
of August 19, 2025.

## Cerebral Blood Flow by Using Pulsed Arterial Spin-Labeling in Elderly Subjects with White Matter Hyperintensities

A.J. Bastos-Leite, J.P.A. Kuijer, S.A.R.B. Rombouts, E.  
Sanz-Arigita, E.C. van Straaten, A.A. Gouw, W.M. van der  
Flier, P. Scheltens and F. Barkhof

*AJNR Am J Neuroradiol* 2008, 29 (7) 1296-1301

doi: <https://doi.org/10.3174/ajnr.A1091>

<http://www.ajnr.org/content/29/7/1296>

ORIGINAL  
RESEARCH

A.J. Bastos-Leite  
J.P.A. Kuijer  
S.A.R.B. Rombouts  
E. Sanz-Arigita  
E.C. van Straaten  
A.A. Gouw  
W.M. van der Flier  
P. Scheltens  
F. Barkhof

# Cerebral Blood Flow by Using Pulsed Arterial Spin-Labeling in Elderly Subjects with White Matter Hyperintensities

**BACKGROUND AND PURPOSE:** On MR imaging, white matter hyperintensities (WMH) on T2-weighted images are generally considered as a surrogate marker of ischemic small vessel disease in elderly subjects. Pulsed arterial spin-labeling (PASL) is a noninvasive MR perfusion-weighted technique. We hypothesized that elderly subjects with diffuse confluent WMH should have lower cerebral blood flow (CBF) measurements than subjects with punctiform or beginning confluent WMH.

**MATERIALS AND METHODS:** MR images of 21 subjects (13 women; mean age, 76 years; SD, 5), stratified for the degree of WMH, from a single center within the multinational Leukoaraiosis and Disability (LADIS) study, were investigated. CBF images were obtained by means of quantitative imaging of perfusion by using a single-subtraction second version, with thin-section TI periodic saturation PASL. Values of cortical gray matter, subcortical (including white matter and deep gray matter), and global CBF were calculated. CBF measurements of subjects with diffuse confluent WMH ( $n = 7$ ) were compared with those of subjects with punctiform or beginning confluent WMH ( $n = 14$ ).

**RESULTS:** Subjects with diffuse confluent WMH were found to have approximately 20% lower mean global CBF (43.5 mL/100 mL/min; SD, 6.3) than subjects with punctiform or beginning confluent WMH (57.9 mL/100 mL/min; SD, 8.6;  $P < .01$ ), as well as approximately 20% lower mean subcortical ( $P < .01$ ) and cortical gray matter CBF ( $P < .05$ ).

**CONCLUSION:** PASL revealed a significant reduction of CBF measurements in elderly subjects with diffuse confluent WMH.

On MR imaging, white matter hyperintensities (WMH) on T2-weighted images, fluid-attenuated inversion recovery (FLAIR) images, and proton density-weighted images are generally considered as a surrogate marker of ischemic small vessel disease in elderly subjects,<sup>1</sup> but their significance is still under debate.

Arterial spin-labeling (ASL) is a functional MR imaging technique that represents an alternative to both nuclear medicine and dynamic susceptibility contrast echo-planar MR imaging (EPI) for the evaluation of cerebral perfusion. By using water as a diffusible tracer, ASL does not require either ionizing radiation or an exogenous contrast bolus injection. Water proton spins in the arterial blood can be inverted (magnetically labeled) before entering the capillary level, after applying an appropriate series of radio-frequency pulses. When these labeled water protons enter the capillary level, they alter the magnetization of the tissue in a way that can be measured

quantitatively.<sup>2</sup> Pulsed ASL (PASL) techniques generally label a large blood volume in a thick slab just below the planes of image acquisition, by inverting the magnetization of water protons with adiabatic hyperbolic secant radio-frequency pulses.<sup>3</sup>

Because WMH most probably represent ischemic small vessel disease,<sup>1,4</sup> we hypothesized that subjects with diffuse confluent WMH should have lower cerebral blood flow (CBF) measurements than subjects with punctiform or beginning confluent WMH. In fact, single-photon emission CT, positron-emission tomography, and dynamic susceptibility contrast perfusion-weighted MR imaging studies have shown that diffuse confluent WMH are associated with reduced cerebral perfusion,<sup>5-7</sup> but most of them did not yield quantification of CBF. To our knowledge, no previous study has shown a relation between different grades of WMH and CBF measurements by means of ASL. Therefore, our purpose was to compare CBF measurements of subjects with diffuse confluent WMH with those of subjects with punctiform or beginning confluent WMH by using PASL.

## Materials and Methods

### Subjects

We included 21 subjects (8 men, 13 women) from a single center within the Leukoaraiosis and Disability (LADIS) study.<sup>8</sup> The current study was approved by both the local and the LADIS study institutional review boards, as well as by the LADIS study steering committee. All subjects gave written informed consent.

The LADIS study is a prospective longitudinal multicenter European study on the role of WMH as an independent predictor for transition to disability in nondemented elderly subjects.<sup>8</sup> Inclusion criteria for the LADIS study were the following: age between 65 and 84

Received November 28, 2007; accepted after revision February 6, 2008.

From the Image Analysis Center (A.J.B.-L., F.B.), VU University Medical Center, Amsterdam, the Netherlands; Alzheimer Center (A.J.B.-L., E.C.v.S., A.A.G., W.M.v.d.F., P.S., F.B.), VU University Medical Center, Amsterdam, the Netherlands; Department of Medical Imaging (A.J.B.-L.), Faculty of Medicine, University of Oporto, Oporto, Portugal; Department of Physics and Medical Technology (J.P.A.K., S.A.R.B.R., E.S.-A.), VU University Medical Center, Amsterdam, the Netherlands; Department of Radiology (S.A.R.B.R.), Leiden Institute for Brain and Cognition, Leiden University Institute for Psychological Research, Leiden University Medical Center, Leiden, the Netherlands; Department of Neurology (E.C.v.S., A.A.G., W.M.v.d.F., P.S.), VU University Medical Center, Amsterdam, the Netherlands; and Department of Radiology (F.B.), VU University Medical Center, Amsterdam, the Netherlands.

Paper previously presented at: 32nd Annual Meeting of the European Society of Neuro-radiology, Genoa, Italy; September 20–23, 2007.

Please address correspondence to António José de Bastos-Leite, MD, University of Oporto, Faculty of Medicine, Department of Medical Imaging, Alameda do Professor Hernâni Monteiro, 4200-319 Oporto, Portugal; e-mail: abastosleite@med.up.pt

DOI 10.3174/ajnr.A1091

years, WMH on MR imaging of any degree according to the Fazekas scale,<sup>9</sup> absence of disability, presence of a regularly contactable informant, and agreement to sign an informed consent. Exclusion criteria were the following: presence of severe illnesses, severe unrelated neurologic diseases, leukoencephalopathy of nonvascular origin, severe psychiatric diseases, inability to give an informed consent, and inability or refusal to undergo cerebral MR imaging.

All subjects underwent an MR imaging examination at baseline. In our center, follow-up MR imaging examinations were performed yearly, and the current report focuses on data obtained during the second or third year of follow-up.

On the basis of clinical findings at the time of undergoing MR imaging, the included subjects for the current study were classified as having normal cognition or cognitive impairment.<sup>10-15</sup> Concurrent medications and drugs possibly influencing CBF were also taken into account.

### MR Imaging Protocol

MR imaging examinations were performed at 1.5T (Sonata; Siemens, Erlangen, Germany) and included axial FLAIR images (TE = 84 ms; TR = 9000 ms; NEX = 2; TI = 2200 ms; FOV = 250 mm; section thickness = 5 mm; number of sections = 24; acquisition matrix = 256 × 192, interpolated to image matrix = 512 × 384) and a high-resolution 3D T1-weighted inversion recovery sequence (TE = 5.17 ms; TR = 2700 ms; TI = 950 ms; flip angle = 8°; NEX = 1; FOV = 250 mm; section thickness = 1 mm; number of sections = 160; acquisition matrix = 256 × 176 [69% FOV phase], interpolated to image matrix = 512 × 352). In addition, to obtain relative CBF (rCBF) images, we chose a quantitative imaging of perfusion by using a single-subtraction second version, with a thin-section TI periodic saturation (Q2TIPS) PASL sequence with proximal inversion and control for off-resonance effects.<sup>16</sup> To convert the signal intensity of the rCBF images to absolute values of CBF, we performed a single-shot EPI sequence of the fully relaxed brain tissue.

### Q2TIPS Tailored to an Elderly Population

ASL techniques rely on subtracting control images (acquired with blood and tissue water in identical magnetization states) from spin-labeled images (acquired with blood and tissue water in different magnetization states). The Q2TIPS variant of PASL enables the acquisition of images in multiple sections and aims to control for 2 major systematic errors of ASL: the variable transit time from the distal edge of the labeled region to the image sections, and the contamination by intravascular signal intensity from labeled blood that flows through the image sections by applying thin-section periodic saturation pulses at the distal end of the labeled region.<sup>16</sup>

We used a 10-cm labeling region, a TE = 15 ms, a TI<sub>1</sub> = 700 ms (time between the inversion pulse and the beginning of periodic saturation pulses), a TI<sub>1</sub> stop time (TI<sub>1s</sub>) = 1600 ms (time between the inversion pulse and the end of periodic saturation pulses), a TI<sub>2</sub> = 1800 ms (time between the inversion pulse and acquisition of the proximal image), and a TR = 2500 ms. By using a TI<sub>2</sub> = 1800 ms, one can obtain an appropriate brain tissue signal intensity in elderly subjects, almost without intravascular signal intensity.<sup>17</sup> To further improve suppression of intravascular signal intensity, we additionally used a bipolar crusher gradient. The sequence was repeated 200 times, alternating between acquisition of 100 labeled and 100 control images (total imaging time = 8.33 minutes), and prospective motion correction<sup>18</sup> was applied before subtracting each labeled-control pair. After subtraction, the difference images were averaged to obtain rCBF im-

ages in 6 sections (FOV = 224 mm, section thickness = 6 mm, inter-section gap = 1.5 mm, matrix = 64 × 64, ascending section acquisition order).

### Quantification of CBF

Quantification of CBF by means of ASL is based on the difference in longitudinal magnetization ( $\Delta M$ ) between labeled and control images. For Q2TIPS,  $\Delta M$  at time  $t = TI_2$  is related to CBF by the following formula<sup>16,19</sup>:

$$1) \quad \Delta M(t = TI_2) = 2fm_a^0 \alpha TI_1 e^{-TI_2/T1_b} \quad \text{for } TI_1 < t_L \text{ and } TI_2 > TI_1 + t_T$$

TI<sub>1</sub> and TI<sub>2</sub> are sequence parameters. TI<sub>b</sub> is the T1 value of arterial blood,  $\alpha$  is the degree of spin inversion,  $m_a^0$  is the arterial blood longitudinal magnetization at equilibrium,  $t_L$  is the time width of the labeling,  $t_T$  is the transit time from the distal edge of the labeled region to the image sections, and  $f$  corresponds to absolute values of CBF. We assumed that TI<sub>1</sub> should be  $< t_L$  and that TI<sub>2</sub> should be  $> TI_1 + t_T$  to obtain valid CBF measurements. In addition, we assumed TI<sub>b</sub> = 1400 ms and  $\alpha = 0.97$ .<sup>16,19</sup>

To account for differences in proton density between blood and brain tissue, we assumed an average value (between gray and white matter) of 0.90 for the blood/brain partition coefficient ( $\lambda$ ), which is defined by the following formula<sup>19,20</sup>:

$$2) \quad \lambda = M^0 / m_a^0$$

$M^0$  corresponds to the brain tissue longitudinal magnetization at equilibrium<sup>19</sup> and is related to the magnitude of signal intensity at equilibrium ( $S^0$ ) by the scanner gain  $G$ :

$$3) \quad S^0 = G \cdot M^0 = G \cdot \lambda \cdot m_a^0$$

$S^0$  was determined by using a single-shot EPI sequence of the fully relaxed brain tissue. This single-shot EPI sequence has an EPI readout similar to that of Q2TIPS but does not have any presaturation, labeling, or periodic saturation pulses. In addition, a dead time of 10 seconds was inserted between adjustment pulses of the scanner and the acquisition of images.

Finally, the difference in signal intensity ( $\Delta S$ ) between labeled and control images (signal intensity of rCBF images) is also related to  $\Delta M$  by the scanner gain  $G$ :

$$4) \quad \Delta S = G \cdot \Delta M$$

Combining equations 1, 3, and 4 and additionally accounting for T2\* effects of blood and brain tissue, we calculated a scaling factor  $C$  to determine absolute CBF measurements from  $\Delta S$  and  $S^0$ :

$$5) \quad f = \Delta S \cdot C / S^0$$

Values for T2\* of blood (40 ms) and brain tissue (100 ms, gray and white matter average) were taken from the literature.<sup>21</sup> Using these values and the values of TE, TI<sub>1</sub>, TI<sub>2</sub>, TI<sub>b</sub>,  $\alpha$ , and  $\lambda$  listed above,  $C$  was calculated to be  $11.5 \cdot 10^3$  mL/100 mL/min for the proximal section.

### Image Analysis

A single reader, with more than 5 years of experience, visually rated the degree of WMH on axial FLAIR images. On the basis of the Fazekas scale,<sup>9</sup> WMH were classified into the following categories: punctiform (score 1), beginning confluent (score 2), and diffuse confluent (score 3).

For all the included cases, the rCBF and  $S^0$  image sections were uniformly positioned, parallel to the anterior/posterior commissure

**Table 1: Characteristics of subjects (*n* = 21), CBF measurements in mL/100 mL/min, and WMH score**

Subjects	Sex	Age	Diagnosis	Medication and Drugs	Cortical CBF	Subcortical CBF	Global CBF	WMHT
1	F	73	—	Diuretic	64.1	37.1	50.5	1
2	M	70	—	Diuretic	65.7	38.4	52.1	1
3	F	78	—	—	69.6	40.4	54.8	1
4	F	79	—	Diuretic	68.5	48.6	58.0	1
5	F	76	AD	AA, nicotine	57.6	34.2	44.4	2
6	F	82	AD	$\beta$ -BI	61.6	34.4	46.2	2
7	F	80	—	—	62.1	37.1	47.9	2
8	F	78	—	—	55.5	41.4	47.9	2
9	M	75	—	Diuretic, CA	66.8	39.4	51.4	2
10	F	66	—	AA	70.7	51.5	60.0	2
11	M	73	—	—	72.5	47.8	60.4	2
12	F	70	—	$\alpha$ 2-agonist	81.2	48.1	62.9	2
13	F	70	—	$\beta$ -BI, nitrate	77.1	53.3	64.4	2
14	F	72	—	CA*, nitrate	106.1	60.2	78.9	2
15	M	80	—	$\beta$ -BI, CA	51.3	26.7	36.2	3
16	M	70	—	$\beta$ -BI, CA	48.7	26.9	37.8	3
17	F	84	—	Diuretic, $\beta$ -BI, AA, nitrate	47.6	35.0	40.6	3
18	M	76	VaD	Diuretic, ACE inhibitor	62.3	31.7	40.9	3
19	M	84	—	ACE inhibitor	60.6	35.2	46.3	3
20	M	71	—	Diuretic, $\beta$ -BI	65.3	37.0	49.4	3
21	F	79	—	—	69.1	42.9	53.1	3
Mean (SD)	—	75.5 (5.1)	—	—	65.9 (12.6)	40.3 (8.6)	51.6 (10.1)	2.1 (0.7)

**Note:**—AD indicates Alzheimer disease; VaD, vascular dementia; AA, angiotensin antagonist;  $\beta$ -BI,  $\beta$ -blocker; CA\*, calcium antagonist (\*diltiazem); ACE inhibitor, angiotensin-converting enzyme inhibitor; WMH, white matter hyperintensities; CBF, cerebral blood flow.

† Higher values indicate greater severity.

line, to include the deep gray matter and most of the cerebral white matter. To analyze rCBF and  $S^0$  images, we used a statistical parametric mapping program (SPM5; Wellcome Department of Cognitive Neurosciences, London, UK). For each subject, rCBF and  $S^0$  images were coregistered<sup>22</sup> to the T1-weighted images by using a stepwise coregistration involving first the coregistration of mean EPI images, obtained after averaging all labeled and control images, to the T1-weighted images. Additionally, a segmentation algorithm<sup>23</sup> combining anatomic information and signal intensity was applied to the T1-weighted images to obtain probabilistic gray and white matter maps. After normalization<sup>24,25</sup> to the standard T1-weighted template, gray and white matter probability maps were converted to binary masks.

Because most of WMH are isointense with gray matter on T1-weighted images, the corresponding voxels have higher probability values on the gray matter maps and lower probability values on the white matter maps than voxels representing normal-appearing white matter. Therefore, to reduce misclassification of white matter lesions as gray matter after brain segmentation, we used a lower threshold to obtain white matter binary masks than to obtain gray matter binary masks (ie, voxels with values >40% on the gray matter probability maps were assigned a value 1 on the gray matter binary masks, and voxels with values >20% on the white matter probability maps were assigned a value 1 on the white matter binary masks). The use of a 40% threshold to obtain gray matter binary masks was also planned to minimize partial volume effects of the CSF occurring, particularly in cases with cortical atrophy. On the obtained binary masks, we still created regions of interest either to correctly classify voxels representing lesions (eg, voxels representing white matter lesions misclassified as gray matter) or to exclude nonbrain voxels.

Because both white matter and deep gray matter hyperintensities are considered to represent subcortical ischemic small vessel disease, we decided to combine voxels classified as deep gray matter and voxels classified as white matter into common subcortical binary masks.

The cortical gray matter and subcortical binary masks were multiplied by the normalized rCBF images, as well as global binary masks

obtained after combining all gray matter and white matter. Global binary masks were also multiplied by normalized  $S^0$  images. Then, the average intensity of the product images was taken, and on the basis of equation 5, values of cortical gray matter, subcortical (including white matter and deep gray matter), and global CBF were calculated. For all CBF calculations, we used a global average (combining all gray matter and white matter)  $S^0$  intensity measurement.

### Statistical Analysis

Statistical analysis was performed by means of the Statistical Package for the Social Sciences 11.0 for Windows (SPSS, Chicago, Ill). Subjects with Fazekas score 3 were compared with those with Fazekas score 1 or 2, because there were few subjects with Fazekas score 1 and the sample size was limited. Given that the Shapiro-Wilk *W* test demonstrated normality in the distribution of data, we used the independent-samples Student *t* test to compare continuous variables, such as CBF measurements. To compare proportions, we used the Fisher exact test. The existence of a sex imbalance between the 2 groups analyzed led us to carry out a multiple linear regression analysis, to account for the effect of sex on CBF. Statistical significance was considered when *P* values were < .05.

### Results

Table 1 summarizes clinical and radiologic characteristics of the subjects and shows values of CBF. At the time of undergoing MR imaging for this study, 18 (85.7%) of the 21 subjects had normal cognition. Of the 3 (14.3%) subjects with cognitive impairment, 2 fulfilled diagnostic criteria for Alzheimer disease, and 1, for subcortical ischemic vascular dementia. Concurrent medications and drugs possibly influencing CBF are also displayed.

Although the difference did not reach statistical significance, the proportion of women among subjects with Fazekas score 1 or 2 (78.6%) was much higher than the proportion of women among subjects with Fazekas score 3 (28.6%). No sig-



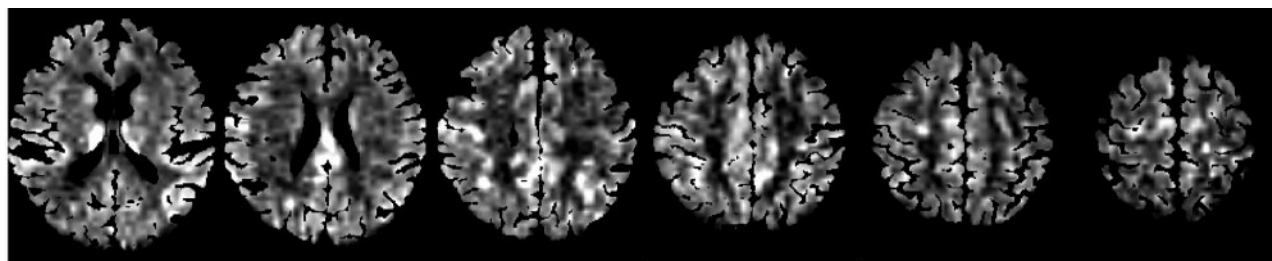


**Fig 1.** CBF images representing the 6 analyzed sections from subject 4.

**Table 2: Comparisons of CBF in mL/100 mL/min between groups of subjects with different grades of WMH**

	Mean CBF (SD)		Relative Difference (%)	P value
	WMH Score 1 or 2 (n = 14)	WMH Score 3 (n = 7)		
Global	55.7 (9.2)	43.5 (6.3)	21.9	<.01
Subcortical	43.7 (7.9)	33.6 (5.8)	23.1	<.01
Cortical	69.9 (12.6)	57.9 (8.6)	17.2	<.05

nificant difference was found between the mean age of subjects with Fazekas score 1 or 2 (74.4 years; SD, 4.6) and the mean age of subjects with Fazekas score 3 (77.7 years; SD, 5.7).

Figure 1 shows global CBF images representing the 6 analyzed sections from a subject with Fazekas score 1. Table 2 shows comparisons of CBF measurements between subjects with Fazekas score 1 or 2 ( $n = 14$ ) and subjects with Fazekas score 3 ( $n = 7$ ). Subjects with Fazekas score 3 were found to have approximately 20% lower mean global, subcortical (including white matter and deep gray matter), and cortical gray matter CBF than subjects with Fazekas score 1 or 2 (Fig 2). The multiple linear regression analysis showed that, after correction for sex, the difference remained statistically significant for global CBF ( $P < .05$ ).

The proportion of subjects under the various types of medications or drugs did not significantly differ between the 2 groups. However, the only subject under therapy with diltiazem, a calcium antagonist with positive inotropic effect, presented with the highest CBF measurements (Table 1, subject 14).

## Discussion

In this study, we determined CBF measurements in elderly subjects with WMH by means of Q2TIPS, a PASL MR perfusion-weighted sequence. Our study indicates that subjects with diffuse confluent WMH have approximately 20% lower CBF measurements than subjects with punctiform or beginning confluent WMH.

So far, few ASL studies have presented absolute values of CBF in elderly subjects<sup>17</sup> or have analyzed CBF measurements in healthy adult subjects, accounting for the effect of age.<sup>26</sup> Considering that CBF quantification by means of ASL techniques is reliable,<sup>26</sup> we found, as in other studies,<sup>17,26</sup> high variation of CBF measurements between subjects.

Although there is no previous report of subcortical CBF values combining white matter and deep gray matter with which to compare, the mean global and cortical gray matter CBF measurements in cases with punctiform or beginning confluent WMH are in agreement with those previously re-

ported for subjects without evidence of WMH. Actually, they are even slightly higher than expected.<sup>17,26</sup> Therefore, subjects with punctiform or beginning confluent WMH do not seem to have considerable brain hypoperfusion. In contrast, subjects with diffuse confluent WMH have global and cortical gray matter CBF values falling below or in the lower range of those previously reported,<sup>17,26</sup> which leads us to consider them as abnormally low.

The cross-sectional design of the current study precludes inferring causality, but the existence of low CBF measurements in subjects with diffuse confluent WMH adds support to the concept that brain hypoperfusion is associated with white matter lesions in the elderly, most probably because of ischemic small vessel disease.<sup>1,4</sup> The existence of histologic evidence of decreased afferent vascular density in WMH, normal-appearing white matter, and cortical gray matter in patients with leukoariosis<sup>27</sup> supports both that concept and our findings. Longitudinal studies may help to clarify whether brain hypoperfusion is a predictor of occurrence or increased severity of WMH and, eventually, of other types of cerebrovascular lesions.

Follow-up results from the entire sample of the LADIS study were published.<sup>28</sup> These results indicate that functionally independent elderly subjects with diffuse confluent WMH are at a considerable risk of becoming dependent in a short period, mostly owing to motor and cognitive deterioration. The demonstration of a considerable hypoperfusion in subjects with diffuse confluent WMH by means of PASL helps to explain the high risk of deterioration in such subjects.

WMH are often associated with Alzheimer disease,<sup>1</sup> and other studies already demonstrated hypoperfusion in patients with Alzheimer disease and mild cognitive impairment by means of ASL.<sup>29-31</sup> In our sample, only 3 patients had the diagnosis of dementia. Although all of these patients presented with low values of CBF, it was not appropriate to compare their CBF measurements with those of the remaining subjects because of insufficient statistical power. Both of our patients with Alzheimer disease had beginning confluent WMH. Their low values of CBF, which may have been the result of mechanisms unrelated to vascular processes, even contradict the global effect that we observed and do not seem to constitute a bias to the major finding of the current study. To our knowledge, no previous ASL study accounted for the effect of WMH in patients with dementia. Therefore, WMH should be a factor to take into account in future studies of brain perfusion involving those patients. Furthermore, PASL may help to clarify the contribution of brain hypoperfusion to cognitive impairment in subjects with or at risk of developing dementia.

White matter CBF measurements by means of ASL may be

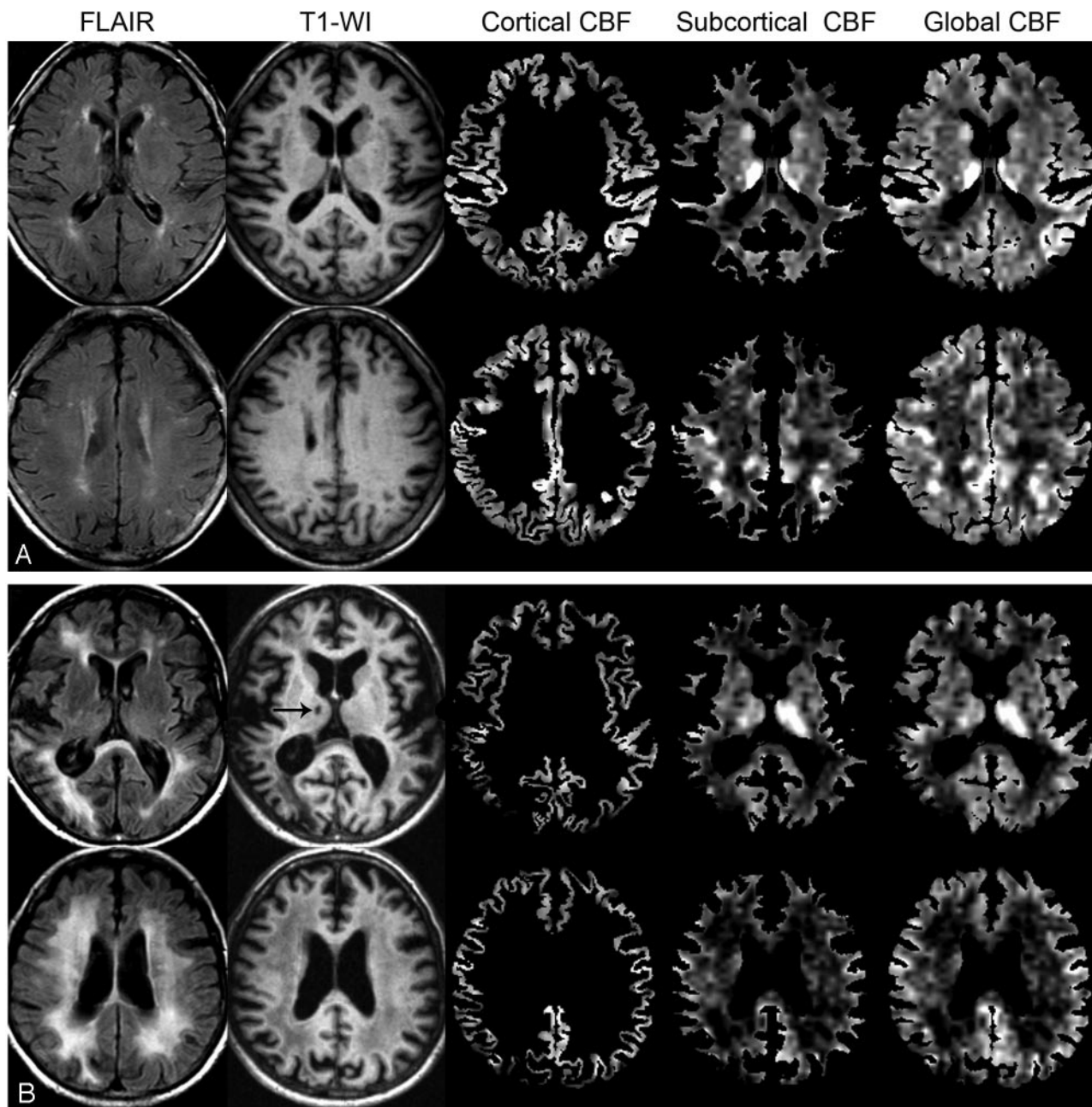


**Fig 2.** A, Axial FLAIR images, T1-weighted images, cortical gray matter CBF images, subcortical CBF images, and global CBF images combining all gray and white matter at the level of the basal ganglia and thalamus (above) and at the level of cerebral white matter (below) from subject 4. B, Corresponding images from subject 18. On the CBF images, note that the cerebral cortex, the cortical-subcortical transition, and the thalamus are highly perfused structures. Also note the perfusion differences between subject 18 (with diffuse confluent WMH on FLAIR images) and subject 4 (with punctiform WMH on FLAIR images). Finally, on the subcortical and global CBF images from subject 18, note the relative hypoperfusion of the right thalamus, where a lacunar infarct occurs (arrow).

problematic, due to a low signal intensity-to-noise ratio. Additionally, arterial transit times in the white matter can be significantly longer than those for gray matter, especially in vascular borderzones. Campbell and Beaulieu<sup>17</sup> suggested 1800 ms as a reasonable postlabel delay time for elderly subjects, and this served as the rationale to use a  $TI_2 = 1800$  ms in the current study. However, given that the mean age of our sample was slightly older than that of their study and because vascular abnormalities occurring in subjects with diffuse confluent WMH may be associated with longer arterial arrival times, it is quite plausible that a  $TI_2 = 1800$  ms may not have

been sufficiently long to be confident that all of the labeled blood could reach the brain tissue. Therefore, our CBF measurements may have been underestimated, especially in subjects with diffuse confluent WMH.

A potential confounder of the current study is the existence of a sex imbalance between the 2 groups analyzed. Given that a previous study has shown that women have approximately 13% higher CBF than men at a given age,<sup>26</sup> it is possible that the results of our study may be, in part, a reflection of the fact that the proportion of men in the group of subjects with diffuse confluent WMH was higher than that in the group with

punctiform or beginning confluent WMH. However, the difference for global CBF remained statistically significant, even after correction for sex. Another potential confounder is that the observed effect may have also been driven by differences in medications and drugs, but the proportion of subjects receiving the various types of medications or drugs possibly influencing CBF did not significantly differ between the 2 groups.

A limitation of the current study is the absence of healthy elderly control subjects without WMH. Given that our sample was taken from the LADIS study,<sup>8</sup> which only recruited subjects with WMH, we were unable to determine values of CBF from age-matched controls without WMH. However, according to large population-based and community-dwelling studies on the prevalence of WMH, subjects without WMH represent no more than approximately 5% of the elderly.<sup>4,32</sup> Other limitations are the small sample size, the absence of control for the presence and degree of flow-limiting carotid stenoses, and the relatively poor signal intensity-to-noise ratio and low spatial resolution of the acquired rCBF and  $S^0$  images. Because of their low spatial resolution, we decided to analyze rCBF and  $S^0$  images globally, by using a statistical parametric mapping program, instead of taking CBF measurements from regions of interest, such as from regions representing the white matter lesions or normal-appearing white matter. In future studies, the acquisition of images with higher spatial resolution, by means of higher field strengths, may allow further investigation of this issue. Nevertheless, because we found a significant reduction of subcortical (including white matter and deep gray matter), cortical gray matter, and global CBF values in subjects with diffuse confluent WMH, it seems that such subjects have indeed a generalized cerebrovascular disease process rather than one confined to lesions.<sup>27</sup>

## Conclusion

PASL enabled us to demonstrate a significant reduction of CBF in elderly subjects with diffuse confluent WMH.

## References

- Scheltens P, Barkhof F, Valk J, et al. White matter lesions on magnetic resonance imaging in clinically diagnosed Alzheimer's disease: evidence for heterogeneity. *Brain* 1992;115(Pt 3):735–48
- Williams DS, Detre JA, Leigh JS, et al. Magnetic resonance imaging of perfusion using spin inversion of arterial water. *Proc Natl Acad Sci U S A* 1992;89:212–16
- Barbier EL, Lamalle L, Decorps M. Methodology of brain perfusion imaging. *J Magn Reson Imaging* 2001;13:496–520
- Longstreth WT Jr, Manolio TA, Arnold A, et al. Clinical correlates of white matter findings on cranial magnetic resonance imaging of 3301 elderly people: The Cardiovascular Health Study. *Stroke* 1996;27:1274–82
- Starkstein SE, Sabe L, Vazquez S, et al. Neuropsychological, psychiatric, and cerebral perfusion correlates of leukoaraiosis in Alzheimer's disease. *J Neurol Neurosurg Psychiatry* 1997;63:66–73
- Yamauchi H, Fukuyama H, Nagahama Y, et al. Brain arteriolosclerosis and hemodynamic disturbance may induce leukoaraiosis. *Neurology* 1999;53:1833–38
- Markus HS, Lythgoe DJ, Ostegaard L, et al. Reduced cerebral blood flow in white matter in ischaemic leukoaraiosis demonstrated using quantitative exogenous contrast based perfusion MRI. *J Neurol Neurosurg Psychiatry* 2000;69:48–53
- Pantoni L, Basile AM, Pracucci G, et al. Impact of age-related cerebral white matter changes on the transition to disability: the LADIS study—rationale, design and methodology. *Neuroepidemiology* 2005;24:51–62
- Fazekas F, Chawluk JB, Alavi A, et al. MR signal abnormalities at 1.5 T in Alzheimer's dementia and normal aging. *AJR Am J Roentgenol* 1987;149:351–56
- Petersen RC, Smith GE, Waring SC, et al. Mild cognitive impairment: clinical characterization and outcome. *Arch Neurol* 1999;56:303–08
- McKhann G, Drachman D, Folstein M, et al. Clinical diagnosis of Alzheimer's disease: report of the NINCDS-ADRDA Work Group under the auspices of Department of Health and Human Services Task Force on Alzheimer's Disease. *Neurology* 1984;34:939–44
- Roman GC, Tatemichi TK, Erkinjuntti T, et al. Vascular dementia: diagnostic criteria for research studies—Report of the NINDS-AIREN International Workshop. *Neurology* 1993;43:250–60
- Erkinjuntti T, Inzitari D, Pantoni L, et al. Research criteria for subcortical vascular dementia in clinical trials. *J Neural Transm Suppl* 2000;59:23–30
- McKeith IG, Galasko D, Kosaka K, et al. Consensus guidelines for the clinical and pathologic diagnosis of dementia with Lewy bodies (DLB): report of the consortium on DLB international workshop. *Neurology* 1996;47:1113–24
- Neary D, Snowden JS, Gustafson L, et al. Frontotemporal lobar degeneration: a consensus on clinical diagnostic criteria. *Neurology* 1998;51:1546–54
- Luh WM, Wong EC, Bandettini PA, et al. QUIPSS II with thin-slice T11 periodic saturation: a method for improving accuracy of quantitative perfusion imaging using pulsed arterial spin labeling. *Magn Reson Med* 1999;41:1246–54
- Campbell AM, Beaulieu C. Pulsed arterial spin labeling parameter optimization for an elderly population. *J Magn Reson Imaging* 2006;23:398–403
- Kuijter JP, Thesen S, Müller E. Pulsed ASL using FOCI pulses combined with prospective motion correction. *Proc Intl Soc Mag Reson Med* 2003;11:664
- Parkes LM, Tofts PS. Improved accuracy of human cerebral blood perfusion measurements using arterial spin labeling: accounting for capillary water permeability. *Magn Reson Med* 2002;48:27–41
- Roberts DA, Rizi R, Lenkinski RE, et al. Magnetic resonance imaging of the brain: blood partition coefficient for water—application to spin-tagging measurement of perfusion. *J Magn Reson Imaging* 1996;6:363–66
- Buxton RB, Frank LR, Wong EC, et al. A general kinetic model for quantitative perfusion imaging with arterial spin labeling. *Magn Reson Med* 1998;40:383–96
- Collignon A, Maes F, Delaere D, et al. Automated multi-modality image registration using information theory. In: Bizais Y, Barillot C, Di Paola R, eds. *Information Processing in Medical Imaging*. Dordrecht, The Netherlands: Kluwer Academic Publishers; 1995:263–74
- Ashburner J, Friston KJ. Unified segmentation. *Neuroimage* 2005;26:839–51
- Ashburner J, Neelin P, Collins DL, et al. Incorporating prior knowledge into image registration. *Neuroimage* 1997;6:344–52
- Ashburner J, Friston KJ. Nonlinear spatial normalization using basis functions. *Hum Brain Mapp* 1999;7:254–66
- Parkes LM, Rashid W, Chard DT, et al. Normal cerebral perfusion measurements using arterial spin labeling: reproducibility, stability, and age and gender effects. *Magn Reson Med* 2004;51:736–43
- Moody DM, Thore CR, Anstrom JA, et al. Quantification of afferent vessels shows reduced brain vascular density in subjects with leukoaraiosis. *Radiology* 2004;233:883–90
- Inzitari D, Simoni M, Pracucci G, et al. Risk of rapid global functional decline in elderly patients with severe cerebral age-related white matter changes: the LADIS study. *Arch Intern Med* 2007;167:81–88
- Alsop DC, Detre JA, Grossman M. Assessment of cerebral blood flow in Alzheimer's disease by spin-labeled magnetic resonance imaging. *Ann Neurol* 2000;47:93–100
- Johnson NA, Jahng GH, Weiner MW, et al. Pattern of cerebral hypoperfusion in Alzheimer disease and mild cognitive impairment measured with arterial spin-labeling MR imaging: initial experience. *Radiology* 2005;234:851–59
- Du AT, Jahng GH, Hayasaka S, et al. Hypoperfusion in frontotemporal dementia and Alzheimer disease by arterial spin labeling MRI. *Neurology* 2006;67:1215–20
- de Leeuw FE, de Groot JC, Achten E, et al. Prevalence of cerebral white matter lesions in elderly people: a population based magnetic resonance imaging study—The Rotterdam Scan Study. *J Neurol Neurosurg Psychiatry* 2001;70:9–14